

# The Near-infrared Optimal Distances Method Applied to Galactic Classical Cepheids Tightly Constrains Mid-infrared Period–Luminosity Relations

Shu Wang<sup>1</sup>, Xiaodian Chen<sup>2</sup>, Richard de Grijs<sup>1,3,4</sup>, and Licai Deng<sup>2</sup>

## ABSTRACT

Classical Cepheids are well-known and widely used distance indicators. Since distance and extinction are usually degenerate, it is important to develop suitable methods to robustly anchor the distance scale. Here, we introduce a near-infrared (near-IR) optimal distance method to determine both the extinction values of and distances to a large sample of 289 Galactic classical Cepheids. The overall uncertainty in the derived distances is less than 4.9%. We compare our newly determined distances to the Cepheids in our sample with previously published distances to the same Cepheids with *Hubble Space Telescope* parallax measurements and distances based on the IR surface brightness method, Wesenheit functions, and the main-sequence fitting method. The systematic deviations in the distances determined here with respect to those of previous publications is less than 1–2%. We hence constructed Galactic mid-IR period–luminosity (PL) relations for classical Cepheids in the four Wide-Field Infrared Survey Explorer (*WISE*) bands ( $W1$ ,  $W2$ ,  $W3$ , and  $W4$ ) and the four *Spitzer* Space Telescope bands ( $[3.6]$ ,  $[4.5]$ ,  $[5.8]$  and  $[8.0]$ ). Based on our sample of hundreds of Cepheids, the *WISE* PL relations have been determined for the first time; their dispersion is approximately 0.10 mag. Using the currently most complete sample, our *Spitzer* PL relations represent a significant improvement in accuracy, especially in the  $[3.6]$  band which has the smallest dispersion (0.066 mag). In addition, the average mid-IR extinction curve for Cepheids has been obtained:  $A_{W1}/A_{K_s} \approx 0.560$ ,  $A_{W2}/A_{K_s} \approx 0.479$ ,  $A_{W3}/A_{K_s} \approx 0.507$ ,  $A_{W4}/A_{K_s} \approx 0.406$ ,  $A_{[3.6]}/A_{K_s} \approx 0.481$ ,  $A_{[4.5]}/A_{K_s} \approx 0.469$ ,  $A_{[5.8]}/A_{K_s} \approx 0.427$ , and  $A_{[8.0]}/A_{K_s} \approx 0.427$  mag.

---

<sup>1</sup>Kavli Institute for Astronomy and Astrophysics, Peking University, Beijing 100871, China; shuwang@pku.edu.cn

<sup>2</sup>Key Laboratory for Optical Astronomy, National Astronomical Observatories, Chinese Academy of Sciences, Beijing 100012, China; chenxiaodian@nao.cas.cn

<sup>3</sup>Department of Astronomy, Peking University, Beijing 100871, China

<sup>4</sup>International Space Science Institute–Beijing, Beijing 100190, China

*Subject headings:* distance scale — stars: variables: Cepheids — infrared: ISM  
— ISM: extinction

## 1. Introduction

Classical Cepheids are well-known and widely used distance indicators in relation to the well-established period–luminosity (PL) relation (the ‘Leavitt law’; Leavitt & Pickering 1912). By employing the PL relation, Cepheids can be used to measure nearby extragalactic distances, constrain the Hubble constant, and study Galactic structure and kinematics. Since Cepheids are sparsely distributed throughout the Galaxy, they suffer from distinct reddening effects for each sightline. Their apparent magnitudes are therefore generally reddened and attenuated by intervening interstellar dust to varying extents (Madore et al. 2017). Determining the empirical PL relations for Galactic Cepheids requires measuring their distances and corrections for the wavelength-dependent extinction effects pertaining to individual Cepheids. However, distance and extinction are often tightly coupled.

Before determining Cepheid distances, the wavelength-dependent extinction values need to be measured for individual Cepheids. To reduce the influence of extinction, multi-band photometry is usually employed to obtain reddening-free magnitudes, such as the widely used Weisenheit functions,  $W = V - R_V(B - V)$  and  $W = V - R_I(V - I)$  (Madore 1976, 1982; Madore & Freedman 1991; Fouqué et al. 2007; Turner 2010). For a constant value of  $R_V$  or  $R_I$ , Weisenheit magnitudes can be derived directly for Cepheid distance measurements. However, adopting constant  $R_V$ ,  $R_I$  values means that we implicitly assume that the optical reddening law is universal. Yet, the optical extinction law, usually expressed as  $A_\lambda/A_V$  at  $\lambda < 0.7 \mu\text{m}$ , is known to vary significantly among sightlines (Cardelli et al. 1989; hereafter CCM). CCM found that the variation can be described by the optical total-to-selective extinction ratio  $R_V = A_V/E(B - V)$ . The average extinction law for diffuse, low-density regions in the Galaxy is  $R_V = 3.1$ , which is commonly used to correct observations for dust extinction. In fact, the optical extinction law exhibits significant diversity even within small regions (in angular size) of the diffuse interstellar medium (Wang et al. 2017). Therefore, Weisenheit functions cannot be applied to dense environments.

The influence of extinction in near-infrared (IR) bands is much less than that in optical bands, e.g.,  $A_J/A_V = 0.29$ ,  $A_{K_s}/A_V = 0.12$  for the average extinction law of Galactic diffuse regions, adopting  $R_V = 3.1$ . The near-IR ratio of total-to-selective extinction, such as  $A_{K_s}/E(H - K_s)$  or  $A_J/E(J - K_s)$ , has been adopted to determine the near-IR extinction and distances to Cepheids. However, the  $A_{K_s}/E(H - K_s)$  values still show variations. The interstellar extinction law toward the Galactic Center determined by Nishiyama et al. (2006)

is  $A_{K_s}/E(H - K_s) = 1.44 \pm 0.01$ ; Nishiyama et al. (2009) determined  $A_{K_s}/E(H - K_s) = 1.61 \pm 0.04$ . This will cause at least a 10% distance uncertainty, which is a key problem in studying the structure of the Galactic bulge.

With independent access to Cepheid distances, the empirical PL relation can be determined directly by fitting the period versus absolute magnitude trends in different filters. In the last century, optical *BVI*-band photometry was usually used to constrain the PL relation (Madore & Freedman 1991; Gieren et al. 1998; Tammann et al. 2003; and references therein). However, the empirical PL relation has an intrinsic dispersion which is caused by the finite width of the instability strip for pulsating stars. This dispersion is particularly significant in optical bands (e.g., in the *B* filter it amounts to  $\sim 0.2$  mag), but it decreases toward longer wavelengths (e.g., in near-IR and mid-IR band, the dispersion is  $< \sim 0.1$  mag; see, e.g., Madore & Freedman 1991; Inno et al. 2013; Gaia Collaboration 2017; and references therein). Therefore, compared with the optical bands, the PL relations in near-IR bands exhibit less dispersion and fewer systematic errors (Madore & Freedman 1991; Gieren et al. 1998; Fouqué et al. 2007; Monson & Pierce 2011). In the past decade, with the wealth of available near-IR photometry for Galactic Cepheids, there have been major improvements in constraining the near-IR Cepheid PL relations (An et al. 2007; Fouqué et al. 2007; Monson & Pierce 2011; Chen et al. 2015, 2017). More recently, and considering that the effects of dust extinction in mid-IR bands are less significant than in near-IR bands, we have seen an increase in interest in mid-IR PL relations (Marengo et al. 2010; Ngeow 2012; Monson et al. 2012). However, more Cepheids samples with accurate distances are needed to reduce the remaining uncertainties in the Galactic mid-IR PL relations.

In this paper, we have collected a large sample of Galactic classical Cepheids with IR data. Their distances have been determined accurately by carefully revisiting the near-IR extinction (Section 2). Mid-infrared PL relations for these Cepheids in the four *Spitzer* and four *WISE* bands are also derived in Section 3. Comparisons of the PL relations and an assessment of the mid-IR extinction law are discussed in Section 4. We summarize our principal conclusions in Section 5.

## 2. Distances to the Galactic Classical Cepheids

### 2.1. Sample and Method

In order to accurately determine the distances to Galactic classical Cepheids in near-IR bands, a sample of Galactic classical Cepheids with near-IR *J*, *H*, *K<sub>s</sub>*-band mean magnitudes has been collected from the literature. Van Leeuwen et al. (2007) published 229 Cepheids

with near-IR mean magnitudes in the South African Astronomical Observatory (SAAO) system. A sample of Galactic Cepheids with individual Baade–Wesselink distances was compiled from publications by Fouqué et al. (2007), Groenewegen (2008), Pedicelli et al. (2010), and Storm et al. (2011). Monson & Pierce (2011) provided near-IR photometric measurements for 131 northern Galactic classical Cepheids. Chen et al. (2017) used 31 open cluster Cepheids to obtain  $JHK_s$  Galactic Cepheid PL relations. After removing duplicate sources, our final sample comprises 289 classical Cepheids.  $J, H, K_s$ -band mean magnitudes in the SAAO and European Southern Observatory (ESO) systems were converted to the Two Micron All Sky Survey ( $2MASS$ ; Skrutskie et al. 2006) system using the color transformation equations given on the  $2MASS$  website <sup>1</sup>. The objects’ names, pulsation periods, and  $J, H, K_s$ -band mean magnitudes are summarized in the first five columns of Table 1.

Table 1:  $2MASS$  and  $WISE$  mean magnitudes and distances for our sample of 289 Galactic Cepheids<sup>a</sup>

Cepheid	$\log(P)$ [d]	$\langle J \rangle$ (mag)	$\langle H \rangle$ (mag)	$\langle K_s \rangle$ (mag)	$\langle W1 \rangle$ (mag)	$\langle W1 \rangle$ (mag)	$\langle W3 \rangle$ (mag)	$\langle W4 \rangle$ (mag)	$\langle \mu_0 \rangle$ (mag)
S VUL	1.839	5.410(0.012)	4.806(0.011)	4.586(0.015)	4.409(0.150)	4.011(0.179)	4.240(0.035)	4.169(0.045)	12.787 $\pm$ 0.086
GY SGE	1.714	5.530(0.012)	4.827(0.011)	4.546(0.015)	4.368(0.098)	3.987(0.151)	4.259(0.026)	4.186(0.039)	12.222 $\pm$ 0.082
V1467 CYG	1.687	8.150(0.013)	7.278(0.012)	6.961(0.016)	6.758(0.150)	6.764(0.074)	6.776(0.044)	6.851(0.242)	14.410 $\pm$ 0.127
SV VUL	1.655	4.552(0.012)	4.051(0.011)	3.905(0.016)	3.850(0.141)	3.660(0.114)	3.888(0.058)	3.868(0.033)	11.620 $\pm$ 0.096
V0396 CYG	1.522	6.031(0.012)	5.037(0.011)	4.619(0.016)	4.297(0.164)	3.996(0.142)	4.055(0.022)	3.880(0.075)	11.364 $\pm$ 0.097
...	...	...	...	...	...	...	...	...	...

<sup>a</sup>The entire table is available in the online journal. A portion is shown here for guidance regarding its form and content.

The  $0.9\,\mu\text{m} < \lambda < 3\,\mu\text{m}$  near-IR extinction follows a power law defined by  $A_\lambda \propto \lambda^{-\alpha}$ , with the index  $\alpha$  spanning a small range of  $1.61 < \alpha < 1.80$  (Draine 2003). However, some of the most recently published values of  $\alpha$  have tended to become systematically larger, even reaching  $\alpha > 2.0$  (Wang & Jiang 2014). The widely adopted extinction laws of CCM, Rieke & Lebofsky (1985), and Weingartner & Draine (2001) are all characterized by  $\alpha = 1.61$ . A steep power law,  $\alpha = 1.99$  (Nishiyama et al. 2006), toward the Galactic Center is also commonly used to correct for extinction in the heavily obscured Galactic bulge. Since our target Cepheids are located nearby in the Galactic plane, we assume  $A_\lambda \propto \lambda^{-1.61}$  ( $\lambda : J, H, K_s$ ) here. The discrepancy in Cepheid distances caused by adopting a larger value of  $\alpha$ ,  $\alpha = 1.99$ , will be discussed in Section 4.1. For each given distance  $d$ , the near-IR extinction is calculated as  $A_\lambda = m_\lambda - M_\lambda - 5 \log d + 5$ , where  $m_\lambda$  is the  $\lambda$ -band mean magnitude and  $M_\lambda$  represents

<sup>1</sup>[http://www.ipac.caltech.edu/2mass/releases/allsky/doc/sec6\\_4b.html](http://www.ipac.caltech.edu/2mass/releases/allsky/doc/sec6_4b.html)

the absolute magnitude (which can be derived from the near-IR PL relations). We adopt the near-IR PL relations of Chen et al. (2017). The discrepancies in Cepheid distances caused by adopting different near-IR PL relations will also be discussed in Section 4.1. In practice, steps of 0.1 pc are adopted for distances in the range  $10 \text{ pc} \leq d \leq 15 \text{ kpc}$ . For a given  $d$ ,  $A_\lambda$  is calculated as  $A_\lambda = m_\lambda - M_\lambda - (5 \log d - 5)$  for  $\lambda = J, H, K_s$ . The most reasonable distance  $d$  results when the extinction values  $A_J$ ,  $A_H$ , and  $A_{K_s}$  can all be fitted by the  $\lambda^{-1.61}$  power law, in a minimum  $\chi^2$  sense. We refer to this method as the near-IR optimal distances method. The accuracy of this method depends on the extinction in the  $J, H, K_s$  bands, which is in essence similar to the construction of the Weisenheit functions, although the latter depend only on two bands (e.g.,  $B, V$  or  $V, I$ ). Therefore, the distances and extinction thus derived are expected to be more reliable.

## 2.2. Distances and Errors

Based on the near-IR optimal distances method described in Section 2.1, the distance moduli of our sample of 289 Galactic Cepheids have been derived. The uncertainty in the distance modulus originates from a few contributors, including the errors in (a) the observed magnitude, (b) the absolute magnitude, and (c) the extinction. In addition, in the application of our method, the  $J, H, K_s$  bands are used simultaneously to determine optimal distances; this introduces (d) a  $\sim 2.0\%$  statistical uncertainty. These uncertainties in the Cepheid distances are tabulated in Table 2. The errors in (a) the observed magnitude come from the photometric uncertainty. The average photometric uncertainty is  $\sim 0.015$  mag in  $J$ ,  $\sim 0.014$  mag in  $H$ , and  $\sim 0.016$  mag in  $K_s$ , which contribute only uncertainties of 0.4% in the distance moduli. Since we use the near-IR PL relations of Chen et al. (2017) to derive the  $J, H, K_s$  absolute magnitudes, we adopt for the uncertainties in the PL relations the errors in (b) these absolute magnitudes, resulting in uncertainties of  $\sim 3.4\%$  uncertainties in the derived distances. The extinction errors are  $\sim 2.2\%$  and come from the uncertainty in the theoretical near-IR extinction law (see for details Section 4.1). Combining these errors, the uncertainties in the optimal distances can be derived. The overall average distance uncertainty, including both systematic and statistical errors, is about 4.9%, with a standard deviation of 1.5%. This is, in fact, an upper limit to the error; the actual distance accuracy is higher: see the discussion in Section 2.3. The values of our derived distance moduli and their uncertainties are tabulated in the last column of Table 1.

Table 2: Error contributions to the uncertainties in the Cepheid distances

Contributor	Uncertainty (%)
(a) Observed magnitude	0.4
(b) Absolute magnitude	3.4
(c) Extinction	2.2
(d) Statistical uncertainty related to our method	2.0
Total	4.9

### 2.3. Comparison with Previously Published Results

To analyze the systematic errors in our distances, we compare our results with independently measured distances from the recent literature: see Fig. 1. A quantitative comparison of the systematic deviations is discussed separately.

We compared our distances with those obtained for the 10 Cepheids which have *Hubble Space Telescope* (*HST*) parallaxes (Benedict et al. 2007), shown in Fig. 1a. The average distance difference between both of our methods is about 1.9%. The most recent Cepheid distances based on the IR surface brightness method were published by Fouqué et al. (2007), Groenewegen (2008), Pedicelli et al. (2010), and Storm et al. (2011). Storm et al.’s (2011) compilation contains 70 Galactic fundamental-mode Cepheids, which includes all Cepheids of both Fouqué et al. (2007) and Groenewegen (2008). Therefore, we compare our Cepheid distances with the results of Storm et al. (2011): see Fig. 1b. The average distance difference between these two methods is about 1.2%. Ngeow (2012) adopted the  $V, I$ -band Wesenheit function to derive individual distances to Galactic Cepheids; the comparison of 228 Cepheid distances is shown in Fig. 1c. The average distance difference between these two methods is about 0.57%. Finally, we compared our distances with open cluster Cepheid distances measured by means of the main-sequence fitting method. The latest results are from Chen et al. (2017). For our comparison, see Fig. 1d. The average distance difference between these two methods is only 0.36%. In summary, the systematic deviation in the resulting distances derived here with respect to previously published values is less than 1–2%. This confirms that our method is indeed very useful in determining individual Cepheid distances.

Note that we did not reject any Cepheids with relative large distance discrepancies when comparing our distances with those published by other authors. For example, in Fig. 1a all data points lie pretty much on the  $y = x$  line, except for FF Aql, which has  $\mu_0$  (*HST*) =  $7.76 \pm 0.14$  mag and  $\mu_0$  (this work) =  $8.00 \pm 0.10$  mag. FF Aql is the brightest star among the classical Cepheids thus far observed with *Gaia*. It has a parallax of  $\varpi_{\text{TGAS}} =$

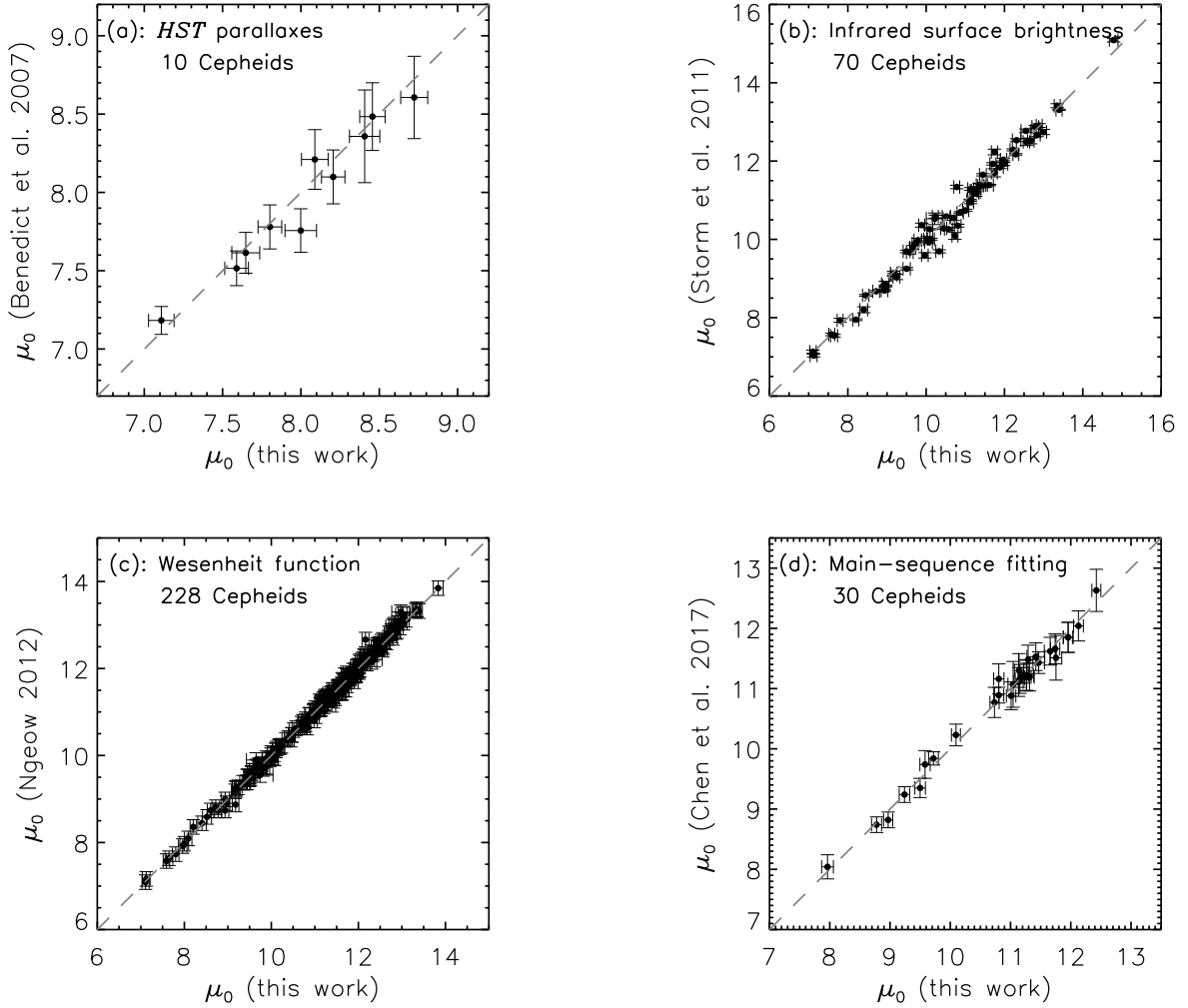


Fig. 1.— Comparison of the distance moduli derived in Section 2.1 (‘this work’) with distance moduli measured based on (a) *HST* parallaxes (10 Cepheids: Benedict et al. 2007); (b) the IR surface brightness method (70 Cepheids: Storm et al. 2011); (c) the Wesenheit function (228 Cepheids: Ngeow 2012); and (d) the main-sequence fitting method (30 Cepheids: Chen et al. 2017). The dashed lines are the  $y = x$  loci and not fits to the data.

$1.640 \pm 0.89$  mas, which is consistent with the object’s measured *HST* parallax to within  $2\sigma$ . This star is, in fact, a binary system and its parallax measurements may therefore be affected by its binary nature. We did not remove it from our sample. However, some studies, including Fouqué et al. (2007) and Ngeow (2012), remove outlier Cepheids from their further discussion. The accuracy of the PL relation depends on the rejection of outliers (Fouqué et al. 2007). Our near-IR optimal distances method can be used to determine distances to a



few thousand Cepheids, and more accurate PL relations could thus be achieved.

### 3. The Galactic Mid-IR Cepheid Period–Luminosity Relations

#### 3.1. The Cepheid Sample with Mid-IR Data

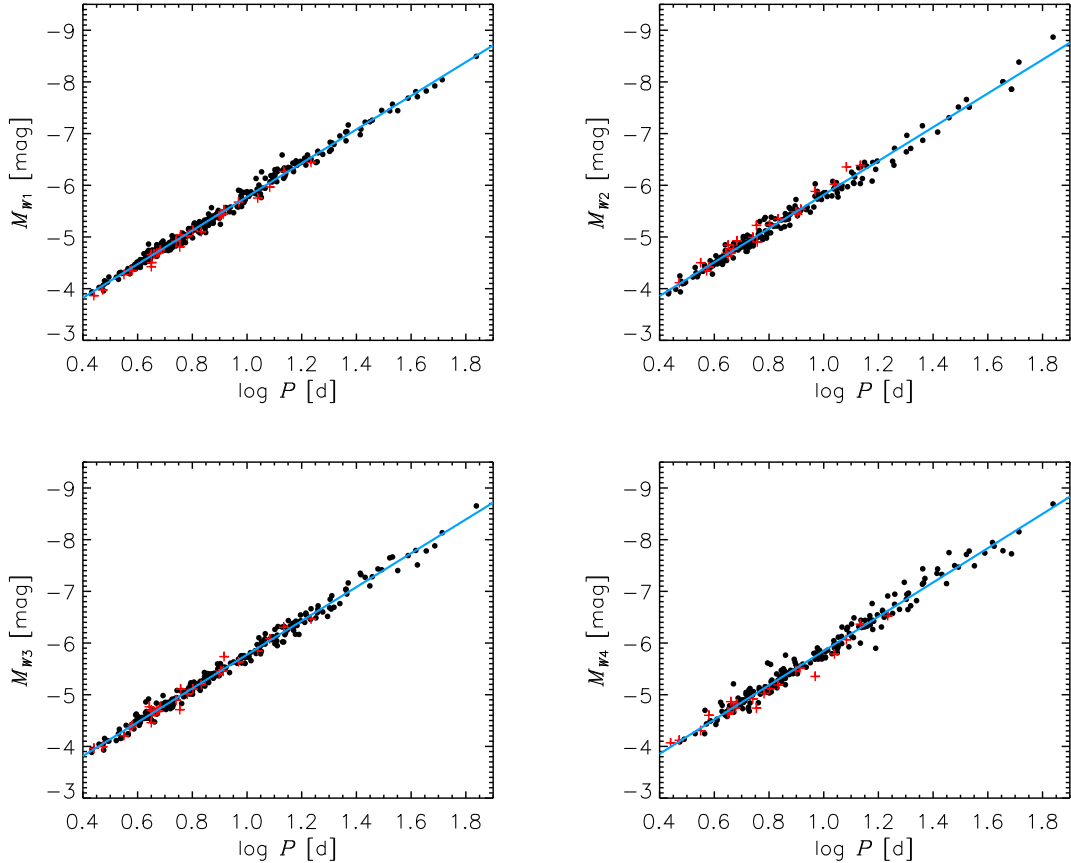


Fig. 2.— *WISE* PL relations with distance moduli listed in Table 1. The black dots are the fundamental-mode classical Cepheids; the red crosses are the first-overtone classical Cepheids; the blue lines are the best-fitting linear results for all Cepheids, including the black dots and red crosses.

Construction of Galactic mid-IR PL relations requires information about the distance and extinction to each Cepheid in one’s sample. The availability of distance moduli pertaining to a large sample (289 Galactic classical Cepheids) offers the possibility to determine accurate mid-IR PL relations. Therefore, we collected the relevant photometric data from *WISE* and *Spitzer* surveys for our sample Cepheids.

The *WISE* survey is a full-sky mid-IR survey with a 40 cm space-borne telescope (Wright



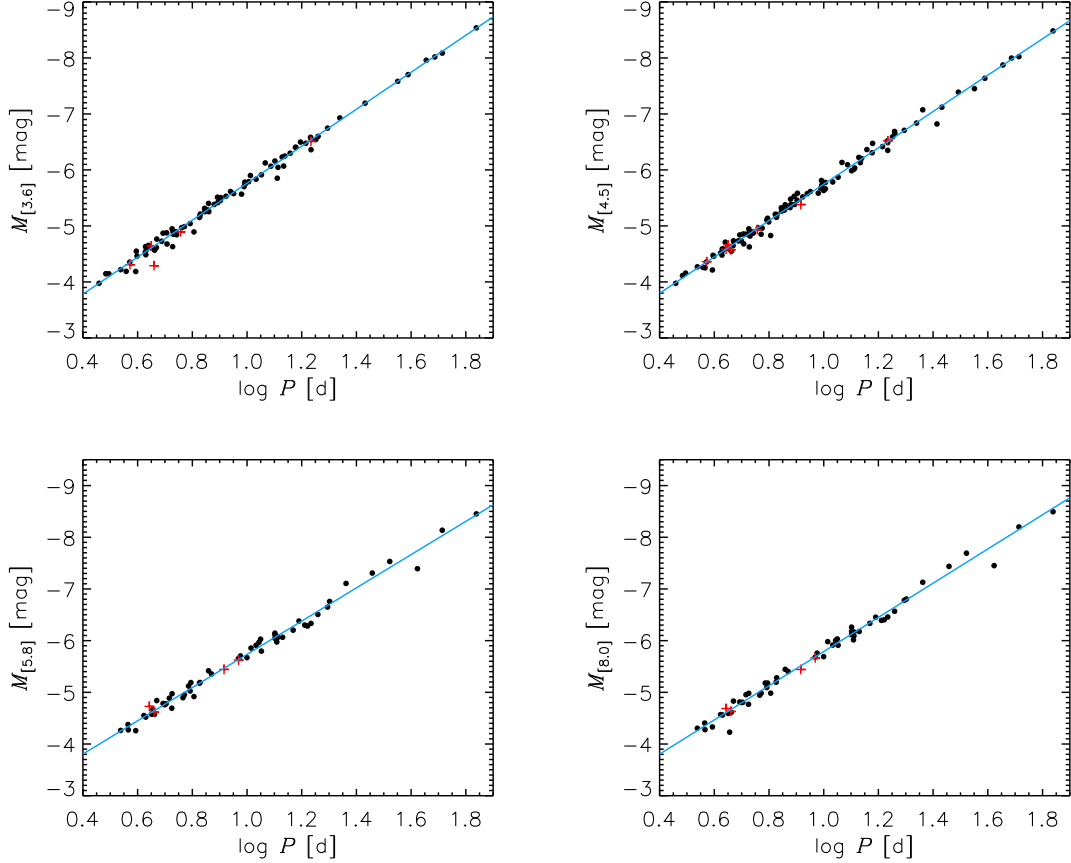


Fig. 3.— As Fig. 2, but for the *Spitzer* bands.

et al. 2010). It mapped the sky in the *W1*, *W2*, *W3*, and *W4* bands (with isophotal central wavelengths of 3.35, 4.60, 11.56, and 22.09  $\mu\text{m}$ , respectively) with  $5\sigma$  limiting magnitudes of about 16.5, 15.5, 11.2, and 7.9 mag, respectively (Wright et al. 2010). We take the *WISE* photometric data of our Cepheid sample from the AllWISE Multi-epoch Photometry Database, which provides time-tagged profile-fit flux measurements for each object in the AllWISE Source Catalog and Reject Table <sup>2</sup>. The numbers of observations taken for each Cepheid are different, ranging from 20 to hundreds of visits. For each Cepheid in our sample, we used contamination and confusion flags (*cc\_flags*) from the AllWISE catalog to reject those data points that may be contaminated or biased in their photometric and/or position measurements. We then calculated the weighted average values in each band by adopting the reciprocal of the measurement square error as weights. Finally, the weighted average values are adopted for the mid-IR *W1*, *W2*, *W3*, and *W4*-band mean magnitudes;

---

<sup>2</sup><http://irsa.ipac.caltech.edu/cgi-bin/Gator/nph-dd>

these latter measurements are also tabulated in Table 1 (sixth to ninth columns).

The Galactic Legacy Infrared Midplane Survey Extraordinaire (GLIMPSE) program is a mid-IR survey in four bands ([3.6], [4.5], [5.8], and [8.0]) using the Infrared Array Camera (IRAC) on board the *Spitzer* Space Telescope. The isophotal central wavelengths are 3.550, 4.439, 5.731, and 7.872  $\mu\text{m}$ , respectively. The survey data include *Spitzer* observations from a number of programs covering the Galactic Plane: GLIMPSE I, GLIMPSE II, GLIMPSE 3D, GLIMPSE 360, Vela-Carina, Deep GLIMPSE, SMOG, and Cygnus-X (Benjamin et al. 2003; Churchwell et al. 2009). We search all catalogs for photometric data of our sample Cepheids. The [3.6], [4.5], [5.8], and [8.0]-band mean magnitudes for each Cepheid in our sample are listed in Table 2. In addition, Monson et al. (2012) used 37 Galactic Cepheids with *Spitzer*/IRAC [3.6] and [4.5]-band photometric measurements to calibrate the Galactic Cepheid PL relations. Their sample covers Cepheid periods ranging from 4 to 70 days. Therefore, we include their Cepheids to supplement the number of objects with  $\log(P) > 1.2$  [days].

Table 3: *Spitzer*/IRAC mean magnitudes for Galactic Cepheids<sup>a</sup>

Cepheid	$\log(P)$ [d]	$\langle[3.6]\rangle$ (mag)	$\langle[4.5]\rangle$ (mag)	$\langle[5.8]\rangle$ (mag)	$\langle[8.0]\rangle$ (mag)
AN AUR	1.012	7.033(0.029)	–	–	–
ER AUR	1.196	8.219(0.039)	–	–	–
YZ AUR	1.260	6.538(0.035)	6.466(0.019)	–	–
AV TAU	0.558	8.397(0.035)	8.300(0.026)	–	–
AX AUR	0.484	9.117(0.037)	9.134(0.025)	–	–
...	...	...	...	...	...

<sup>a</sup>The entire table is available in the online journal. A portion is shown here for guidance regarding its form and content.

In summary, we collected eight-band mid-IR mean magnitudes from the *WISE* and *Spitzer* survey programs. In the *W1*, *W2*, *W3*, and *W4* bands, the total numbers of Cepheids with available mean magnitudes are 283, 215, 287, and 220, respectively. In the [3.6], [4.5], [5.8], and [8.0] bands, the numbers are 91, 107, 59, and 59, respectively.

Table 4: Parameters of the Galactic mid-IR PL Relations

Band ( $\lambda$ )	$N$	$a_\lambda$	$b_\lambda$	$\sigma$
All Cepheids				
$W1$	283	$-3.258 \pm 0.018$	$-2.519 \pm 0.017$	0.082
$W2$	215	$-3.266 \pm 0.027$	$-2.551 \pm 0.026$	0.108
$W3$	287	$-3.270 \pm 0.019$	$-2.505 \pm 0.019$	0.090
$W4$	220	$-3.315 \pm 0.030$	$-2.530 \pm 0.031$	0.123
[3.6]	91	$-3.302 \pm 0.023$	$-2.461 \pm 0.023$	0.066
[4.5]	107	$-3.246 \pm 0.023$	$-2.499 \pm 0.023$	0.071
[5.8]	59	$-3.216 \pm 0.042$	$-2.519 \pm 0.043$	0.097
[8.0]	59	$-3.307 \pm 0.040$	$-2.482 \pm 0.041$	0.091
Excluding First-Overtone Cepheids				
$W1$	256	$-3.248 \pm 0.018$	$-2.533 \pm 0.018$	0.082
$W2$	193	$-3.266 \pm 0.027$	$-2.545 \pm 0.027$	0.107
$W3$	259	$-3.263 \pm 0.020$	$-2.512 \pm 0.020$	0.090
$W4$	198	$-3.317 \pm 0.032$	$-2.534 \pm 0.033$	0.125
[3.6]	86	$-3.298 \pm 0.024$	$-2.467 \pm 0.024$	0.066
[4.5]	100	$-3.245 \pm 0.024$	$-2.502 \pm 0.024$	0.073
[5.8]	55	$-3.222 \pm 0.044$	$-2.511 \pm 0.045$	0.099
[8.0]	55	$-3.311 \pm 0.042$	$-2.479 \pm 0.044$	0.093

### 3.2. Galactic Mid-IR PL Relations

As elaborated by Wang et al. (2014), numerous observations appear to suggest that the mid-IR extinction at  $3\mu\text{m} < \lambda < 8\mu\text{m}$  is  $\sim 0.5$  times lower than in the near-IR  $K_s$  band. The average  $K_s$ -band extinction,  $\langle A_{K_s} \rangle$  for the 289 Cepheids in our sample is 0.17 mag. This implies that the mid-IR extinction is about 0.09 mag, which contributes to propagation of  $\sim 4\%$  uncertainties in distances. Mid-IR extinction corrections should be considered, although they are usually ignored. Because the mid-IR extinction is largely independent of the exact sightline compared with the extinction at shorter wavelengths, we use the average Galactic extinction from Wang et al. (2015) to correct for the mid-IR extinction in this paper.

With the Cepheid distances derived in Section 2.2 and this extinction correction, the absolute magnitudes in the *WISE* and *Spitzer* bands can now be calculated for each Cepheid in our sample. By means of straightforward linear fits to the  $\log P$  versus absolute magnitude

diagrams, the mid-IR PL relations are determined. Figures 2 and 3 show the best-fitting results for the mid-IR *WISE* and *Spitzer* PL relations, respectively. The black dots represent the classical Cepheids, while the blue solid line is our linear fit. The parameters defining our mid-IR multiband PL relations are summarized in Table 4 upper panel as “All Cepheids”. Overall, the statistical errors in our mid-IR PL relations are small. They are less than 0.1 mag except in the *W4* band (0.12 mag).

Note that there are 28 first-overtone Cepheids in our sample of 289 Galactic Cepheids (Section 2.1). Their  $\log P$  ranges from 0.440 to 1.234 [days], with only three of them characterized by  $\log P > 1.0$  [days]. Therefore, we also exclude these objects in our derivations of the mid-IR *WISE* and *Spitzer* PL relations. More specifically, there are 27, 22, 28, and 22 such sources in the *W1*, *W2*, *W3*, and *W4* bands, and five, seven, four, and four of these objects in [3.6], [4.5], [5.8], [8.0] bands, respectively. They are indicated as red crosses in Figs 2 and 3. The parameters of the PL relations based on only the fundamental-mode Cepheids are listed in Table 4. Comparison of these results with those obtained for all Cepheids shows that the slopes and zero points are the same within the uncertainties.

We also investigated whether these mid-IR PL relations may include any possible non-linearities. We adopted a nonparametric regression technique to explore this aspect. In brief, this method allowed us to obtain good fits to the data points without the need for a ‘linear’ assumption (see for details Section 4 of Chen et al. 2016). For the eight mid-IR bands, we analyzed the differences between the nonparametric regression and the linear fit results. The differences are small ( $< 0.03$  mag) and exhibit predominantly random deviations for all eight bands and for all period ranges, which implies that our mid-IR PL relations unlikely contain nonlinear features.

## 4. Discussion

### 4.1. Uncertainties in the Near-IR Optimal Distances Method

Independent Cepheid distances can be obtained from trigonometric parallaxes, the IR surface brightness method, and the main-sequence fitting method. These distances are usually used to determine and constrain the zero points of Cepheid PL relations. Although, distances determined based on the near-IR optimal distances method are indirect distances, by virtue of the large size of our Cepheid sample (289 sources) the overall distance uncertainties are small (see Section 2.2). The near-IR optimal distances method depends on both the near-IR extinction laws and the PL relations. Therefore, we test if our adopted different near-IR theoretical extinction laws or the near-IR PL relations could cause systematic

differences in determining Cepheid distances.

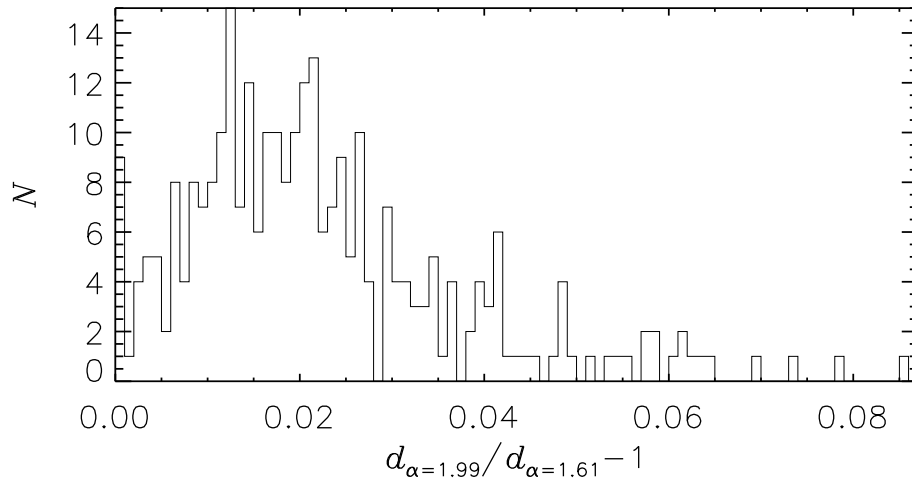


Fig. 4.— Comparison of Cepheid distances determined by adopting different theoretical extinction laws,  $A_\lambda \propto \lambda^{-\alpha}$ , with  $\alpha = 1.61$  or  $1.99$ , to correct our Cepheids for the effects of near-IR extinction.

In Section 2.1, we adopted a power law  $A_\lambda \propto \lambda^{-\alpha}$  with  $\alpha = 1.61$  to correct for the Cepheids’ near-IR extinction. A steeper power law, with an index of  $\alpha = 1.99$ , has also been used to correct for the extinction in the heavily obscured Galactic bulge. Hence, we discuss the discrepancies in Cepheid distances caused by adopting this larger value of  $\alpha$ . The comparison result is shown in Fig. 4. It is apparent that the distances become systematically larger when adopting  $\alpha = 1.99$ . There are 18 Cepheids (6% of the total number of 289 Cepheids) with distance discrepancies in excess of 5%. These Cepheids do not have any specific properties compared with the other Cepheids in our sample. The average distance discrepancy is  $\sim 2.2\%$ , with a standard deviation of  $1.5\%$ . This small systematic error underscores that our distance determination method is reliable, even when considering variations in the interstellar environment.

We have adopted the near-IR PL relations of Chen et al. (2017), which are currently the most complete near-IR Cepheid PL relations, based on 31 open cluster Cepheids with distances determined using the main-sequence fitting method. In our distance uncertainties analysis (Section 2.2), we considered the maximum systematic errors in these PL relations, concluding that they contribute  $\sim 3.4\%$  to the uncertainty in the resulting distances (Table 2). To investigate the effects of adopting different near-IR PL relations, we also use the PL relations of Strom et al. (2011). The distance discrepancy caused by adopting different near-IR PL relations is  $\sim 1.4\%$ , with a standard deviation of  $1.4\%$ , which is less than the

systematic error of 3.4%. This means that the published near-IR PL relations agree well with each other given the prevailing uncertainties, and adopting different PL relations does not measurably affect our distance determination.

#### 4.2. Advantages of Galactic Mid-IR PL Relations

The experiential four-band *WISE* classical Cepheid PL relations were determined for the first time based on our sample of hundreds of Cepheids (see Table 3). These PL relations are characterized by high accuracies. The uncertainties in the mid-IR PL relations are 0.08, 0.1, 0.09, and 0.12 mag in the *W1*, *W2*, *W3*, and *W4* bands, respectively. Compared with the uncertainties in the current near-IR PL relations (e.g., 0.155, 0.146, 0.144 mag in the *J*, *H*, *K<sub>s</sub>* bands: Fouqué et al. 2007; 0.22 mag in the *J*, *K* bands: Strom et al. 2011; 0.148, 0.124, 0.120 mag in the *J*, *H*, *K<sub>s</sub>* bands: Chen et al. 2017; 0.155, 0.146, 0.144 mag in the *J*, *H*, *K* bands: Madore et al. 2017), these mid-IR uncertainties are even smaller. This means that more accurate distances to classical Cepheids could be obtained based on these *WISE* PL relations. The small dispersions of  $< 0.12$  mag in the *WISE* PL relations also underscore the accuracy of the *WISE* photometry of bright classical Cepheids. Since the full-sky *WISE* survey provides multi-epoch photometric data, these PL relations could be used to determine distances to a few thousand Cepheids.

Our *Spitzer* PL relations are based on the largest Cepheid sample available to date: it is composed of triple the number of objects compared with the 29 Cepheids of Ngeow (2012) and twice the number of sources compared with the 37 objects of Monson et al. (2012) with observations in the [3.6] and [4.5] bands. This represents a significant improvement. Compared with previous determinations, the newly derived *Spitzer* PL relations agree well with previously published results based on other methods, given the associated uncertainties, and the accuracy is significantly improved. With respect to the slopes determined by Ngeow (2012), we find differences of 0.060 and 0.066 mag dex<sup>-1</sup> in the [3.6] and [4.5] bands. While our slope of the [3.6] PL relation is consistent (discrepancy: 0.008 mag dex<sup>-1</sup>) with that of Monson et al. (2012), who fixed the slope to  $-3.31$  and determined their [3.6]-band PL relation using *Spitzer* Large Magellanic Cloud data. They calibrated the zero point of the [3.6] PL relation at  $-5.80 \pm 0.03$  mag by relying on the geometric *HST* guide-star distances to 10 Galactic Cepheids. The discrepancy in the *Spitzer* [3.6]-band PL relation’s zero point between our derivation and that of Monson et al. (2012) is only 0.019 mag.

We also compared the *WISE* PL relations with the *Spitzer* PL relations. Since the isophotal wavelengths of the *W1* and *W2* bands are comparable with those of the [3.6] and [4.5] bands, the slopes of our PL relations in these sets of bands are comparable. Among

the mid-IR PL relations in the eight bands available, the *Spitzer* [3.6]-band PL relation has the lowest uncertainty (0.066 mag), which propagates to  $\sim 3\%$  uncertainties in the resulting distances. This uncertainty is smaller than the uncertainties in the Galactic near-IR PL relations (e.g., 0.22 mag: Storm et al. 2011;  $> 0.12$  mag: Chen et al. 2017), and even smaller than the uncertainties in the LMC PL relations ( $> 0.11$  mag in the [3.6] and [4.5] bands: Scowcroft et al. 2011;  $> 0.09$  mag in the  $J, H, K_s$  bands: Macri et al. 2015). It is also smaller than the uncertainties in the SMC PL relations ( $> 0.16$  mag in the IRAC bands: Ngeow & Kanbur 2010;  $> 0.21$  mag in the *AKARI* 3.2  $\mu\text{m}$  and 4.1  $\mu\text{m}$  bands: Ngeow et al. 2012). Moreover, our uncertainty of 0.066 mag provides an upper limit to the width of the Cepheid instability strip.

### 4.3. Mid-IR Extinction

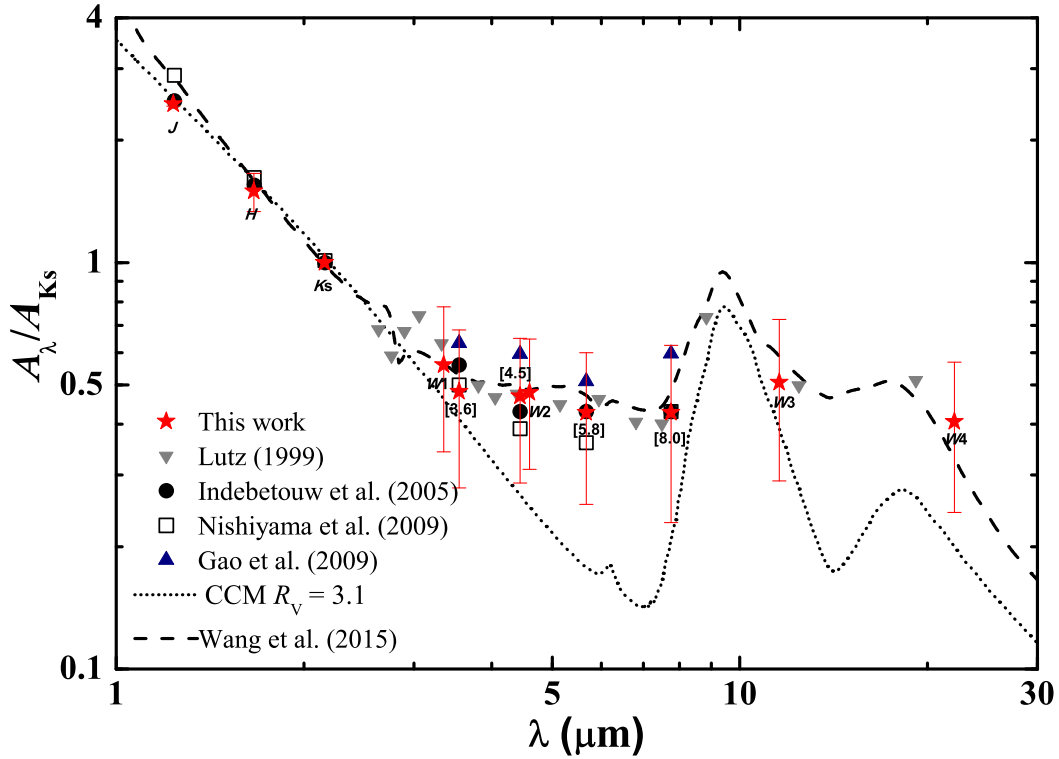


Fig. 5.— Comparison of the extinction derived in this paper (red stars) with previous determinations (different symbols). The CCM  $R_V = 3.1$  model and the Wang et al. (2015) ice model extinction curves are also shown.



Using the mid-IR intensity-averaged magnitudes and multi-band PL relations, we calculate the mid-IR extinction for individual Cepheids. The mean mid-IR extinction values (relative to  $A_{K_s}$ ) in the four *WISE* bands and the four *Spitzer* bands are:  $A_{W1}/A_{K_s} \approx 0.560 \pm 0.218$ ,  $A_{W2}/A_{K_s} \approx 0.479 \pm 0.169$ ,  $A_{W3}/A_{K_s} \approx 0.507 \pm 0.217$ ,  $A_{W4}/A_{K_s} \approx 0.406 \pm 0.163$ ,  $A_{[3.6]}/A_{K_s} \approx 0.481 \pm 0.202$ ,  $A_{[4.5]}/A_{K_s} \approx 0.469 \pm 0.182$ ,  $A_{[5.8]}/A_{K_s} \approx 0.427 \pm 0.173$ , and  $A_{[8.0]}/A_{K_s} \approx 0.427 \pm 0.198$  mag. The results are illustrated in Fig. 5 as red stars. Previous determinations for other lines of sight (e.g., Lutz 1999; Indebetouw et al. 2005; Nishiyama et al. 2009; Gao et al. 2009) are represented by different symbols. For comparison, the CCM  $R_V = 3.1$  model and the Wang et al. (2015) ice model extinction curves are also shown.

## 5. Summary

We have introduced a near-IR optimal distances method to determine the distances to Galactic classical Cepheids. Based on these newly derived distances, the mid-IR PL relations have been tightly constrained. The major results of this paper are as follows:

1. Distances to the overall sample of 289 Galactic classical Cepheids have been determined. The global uncertainty is less than 4.9%.
2. Comparison of our distance moduli with those from literature sources based on *HST* parallaxes, the IR surface brightness method, Wesenheit functions, and the main-sequence fitting method. The average systematic discrepancy between our results and sets of published distances is less than 1–2%.
3. Galactic mid-IR PL relations for Cepheids in the four *WISE* bands (*W1*, *W2*, *W3*, and *W4*) have been constructed for the first time, based on a sample containing hundreds of Cepheids. PL relations in the four *Spitzer*/IRAC bands ([3.6], [4.5], [5.8] and [8.0]) have also been constructed, resulting in significant improvements in the associated uncertainties. Among the published PL relations, our *Spitzer* [3.6]-band PL relation has the smallest dispersion 0.066 mag.
4. The mean mid-IR extinction curve for Cepheids has been obtained:  $A_{W1}/A_{K_s} \approx 0.560$ ,  $A_{W2}/A_{K_s} \approx 0.479$ ,  $A_{W3}/A_{K_s} \approx 0.507$ ,  $A_{W4}/A_{K_s} \approx 0.406$ ,  $A_{[3.6]}/A_{K_s} \approx 0.481$ ,  $A_{[4.5]}/A_{K_s} \approx 0.469$ ,  $A_{[5.8]}/A_{K_s} \approx 0.427$ , and  $A_{[8.0]}/A_{K_s} \approx 0.427$  mag.
5. Finally, based on our sample of 91 Cepheids with [3.6]-band absolute magnitudes, the [3.6]-band PL relation zero point of Freedman et al. (2012) can be well constrained. If we adopt the slope of  $-3.31$  pertaining to the LMC Cepheids, the systematic error in the distance modulus to the LMC is reduced from 0.033 mag to  $0.066/\sqrt{91} = 0.007$

mag. Combining the observational data for 80 LMC Cepheids, a distance modulus of  $\mu_0 = 18.457 \pm 0.011$  (statistical)  $\pm 0.007$  (systematic) mag is obtained. Consequently, the uncertainty in the absolute zero point of the PL relation decreases from 1.7% to 0.3%, and this also means that the zero point of the [3.6]-band PL relation is no longer a major contributor to remaining uncertainty in the Hubble constant.

We thank Noriyuki Matsunaga for very helpful discussions. This work is partially supported by the Initiative Postdocs Support Program (No. BX201600002) and the China Postdoctoral Science Foundation 2017M610998. S. W. acknowledges support from a KIAA Fellowship. R.d.G. is grateful for funding support from the National Natural Science Foundation of China through grants U1631102, 11373010, and 11633005.

## REFERENCES

- An, D., Terndrup, D. M., & Pinsonneault, M. H. 2007, *ApJ*, 671, 1640
- Benedict, G. F., McArthur, B. E., Feast, M. W., et al. 2007, *AJ*, 133, 1810
- Benjamin, R. A., et al. 2003, *PASP*, 115, 953
- Cardelli, J. A., Clayton, G. C., Mathis, J. S. 1989, *ApJ*, 345, 245 (CCM)
- Chen, X. D., de Grijs, R., & Deng, L. C. 2015, *MNRAS*, 446, 1268
- Chen, X. D., de Grijs, R., & Deng, L. C. 2016, *ApJ*, 832, 138
- Chen, X. D., de Grijs, R., & Deng, L. C. 2017, *MNRAS*, 464, 1119
- Churchwell, E., et al. 2009, *PASP*, 121, 213
- Fouqué, P., Arriagada, P., Storm, J., et al. 2007, *A&A*, 476, 73
- Freedman, W. L., Madore, B. F., Scowcroft, V., et al. 2012, *ApJ*, 758, 24
- Gaia Collaboration, Clementini, G., Eyer, L., et al. 2017, *A&A*, in press (arXiv:1705.00688)
- Gao, J., Jiang, B. W., & Li, A. 2009, *ApJ*, 707, 89
- Gieren, W. P., Fouqué, P., & Gómez, M. 1998, *ApJ*, 496, 17
- Groenewegen, M. A. T. 2008, *A&A*, 488, 25
- Indebetouw, R., et al. 2005, *ApJ*, 619, 931
- Inno, L., Matsunaga, N., Bono, G., et al. 2013, *ApJ*, 764, 84
- Leavitt, H. S., & Pickering, E. C. 1912, *Harvard College Obs. Circ.*, 173, 1
- Lutz, D. 1999, in: *The Universe as Seen by ISO*, eds P. Cox & M. Kessler, *ESA Special Publ.*, 427 (Noordwijk: ESA), p. 623
- Macri, L. M., Ngeow, C.-C., Kanbur, S. M., et al. 2015, *AJ*, 149, 117.
- Madore, B. F. 1976, *RGOB*, 182, 153
- Madore, B. F. 1982, *ApJ*, 253, 575
- Madore, B. F., & Freedman, W. L. 1991, *PASP*, 103, 933

- Madore, B. F., Freedman, W. L., & Moak, S. 2017, *ApJ*, 842, 42
- Marengo, M., Evans, N. R., Barmby, P., et al. 2010, *ApJ*, 709, 120
- Monson, A. J., Freedman, W. L., Madore, B. F., et al. 2012, *ApJ*, 759, 146
- Monson, A. J., & Pierce, M. J. 2011, *ApJS*, 193, 12
- Ngeow, C.-C., & Kanbur, S. M., 2010, *ApJ*, 720, 626
- Ngeow, C.-C. 2012, *ApJ*, 747, 50
- Ngeow, C.-C., Citro, D. M., & Kanbur, S. M., 2012, *MNRAS*, 420, 585
- Nishiyama, S., Nagata, T., Kusakabe, N., et al. 2006, *ApJ*, 638, 839
- Nishiyama, S., Tamura, M., Hatano, H., et al. 2009, *ApJ*, 696, 1407
- Pedicelli, S., Lemasle, B., Groenewegen, M., et al. 2010, *A&A*, 518, A11
- Rieke, G. H., & Lebofsky, M. J. 1985, *ApJ*, 288, 618
- Scowcroft, V., Freedman, W. L., Madore, B. F., et al. 2011, *ApJ*, 743, 76
- Skrutskie, M. F., Cutri, R. M., Stiening, R., et al. 2006, *AJ*, 131, 1163
- Storm, J., Gieren, W., Fouqué, P., et al. 2011, *A&A*, 534, A94
- Tammann, G. A., Sandage, A., & Reindl, B. 2003, *A&A*, 404, 423
- Turner, D. G. 2010, *Ap&SS*, 326, 219
- van Leeuwen, F., Feast, M. W., Whitelock, P. A., & Laney, C. D. 2007, *MNRAS*, 379, 723
- Wang, S., & Jiang, B. W. 2014, *ApJ*, 788, L12
- Wang, S., Li, A., & Jiang, B. W. 2015, *MNRAS*, 454, 569
- Wang, S., Jiang, B. W., Zhao, H., Chen, X. D., & de Grijs, R. 2017, *ApJ*, 848, 106
- Weingartner, J. C., & Draine, B. T. 2001, *ApJ*, 548, 296
- Wright, E. L., et al. 2010, *AJ*, 140, 1868